On Peak and Periodic Solutions of an Integro-Differential Equation on S^1

Edith Geigant

Abteilung Theoretische Biologie, Universität Bonn, D-53105 Bonn, Germany
edith.geigant@uni-bonn.de

1 Orientational Models

For the dynamics of an elongated object its orientation is as important as its spatial position; think of a school of fish. Sometimes the orientational pattern alone attracts our attention. In our case it was the phenomenon of parallel bundling and orthogonal arrangement in networks of actin filaments. Actin is a filamentous (i.e. lengthy) protein which forms one of the main components of the cytoskeleton, giving the cell mechanical stability and the ability to crawl ([1]).

Orientational aggregation of filaments can be modeled by a stochastic jump process with interaction ([12]). Here we analyze the approximating mean field equation for orientational dynamics. Let $f(t,\theta)$ be the mean density distribution of filaments (e.g. actin) at time $t \geq 0$ over their orientation $\theta \in S^1 = \mathbb{R}/\mathbb{Z}$ (note our normalization vol$S^1 = 1$). We consider the following integro-differential equation for the temporal evolution of f, using the notation $\dot{f}(\theta) = \partial_t f(.,\theta)$:

$$\dot{f}(\theta) = -\int_{S^1} W[f](\theta,\psi) f(\theta)\, d\psi + \int_{S^1} W[f](\psi,\theta) f(\psi)\, d\psi \tag{1}$$

where

$$W[f](\theta,\psi) = \int_{S^1} h(\phi-\theta)\, G_\sigma(\psi-\theta-v(\phi-\theta))\, f(\phi)\, d\phi\,.$$

For a filament with orientation θ the 'turning rate' $W[f](\theta,\psi)$ is the probability of jumping to location ψ, given the distribution f. So the first term in (1) (with a minus sign) accumulates all the filaments jumping away from orientation θ, and the second term (with a plus sign) accumulates all filaments jumping into orientation θ.

A filament at θ interacting with a filament at ϕ changes its orientation instantly to ψ, see Figure 1. Since the turning mechanism is invariant to rotations, ψ is chosen relative to θ and ϕ. The preferred value of ψ is the *optimal turning angle* $v(\phi-\theta)$. The variation around this angle is described by a periodic Gaussian $G_\sigma : S^1 \to \mathbb{R}_+$ with standard deviation $\sigma > 0$,

$$G_\sigma(\psi) = \frac{1}{\sqrt{2\pi}\sigma} \sum_{n\in\mathbb{Z}} e^{-\frac{1}{2}(\frac{\psi+n}{\sigma})^2},$$

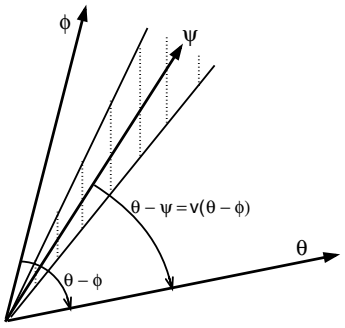

Fig. 1. Sketch of orienting filaments.

i.e. σ measures the *inaccuracy* of turning. The *interaction rate* $h : S^1 \to \mathbb{R}_+$ is an even and the optimal turning angle $v : S^1 \to S^1$ is an odd function of the interaction angle $\phi - \theta$, which follows from the assumption that the filaments cannot distinguish between left and right; they only can take into account angular differences. In mathematical terms: We have not only $SO(2)$ as symmetry group, i.e. solutions are invariant to rotations, but even $O(2)$, i.e. solutions may be also reflected.

The biological motivation is that orientational patterns of actin filaments are mediated by so-called actin binding proteins. Thus, h represents the binding rate of these proteins to actin, v describes the turning mechanism, e.g. favoring parallel alignment or orthogonal configuration, and G_σ models random deviations from the optimal resultant angle. The original non-periodic version of this equation was invented to model the distribution of dominance in insect colonies, [8]. It was applied to actin dynamics in [4]. Other models on actin dynamics use partial integro-differential equations, where the partial derivative is (orientational) diffusion and the integrals describe jumping and binding to filaments in favorable (relative) orientations, see [2] and [13] for modeling aspects, [9] and [10] for mathematical analysis (also in 3D), and [11] for a simplified spatio-angular model.

2 Bundles and Networks

The mass $\int f = \int_{S^1} f(\theta)\, d\theta$ is preserved. We rescale time and f to get $\int f = 1$ and $\int h = 1$. We assume that $h \in \mathrm{L}^2(S^1)$ and v is measurable. Then there exist unique square-integrable solutions of (1), see [5]. Given a non-negative initial distribution, the solution is strictly positive for all times $t > 0$, because the deviation $G_\sigma > 0$ distributes filaments to any orientation (see [5] for a proof for continuous solutions).

Fourier transformation of equation (1) leads to an infinite system of ODEs (subscripts denote Fourier coefficients):

$$\dot{f}_l = \sum_{k\in\mathbb{Z}} w_{l,k}\, f_k f_{l-k} \tag{2}$$

with

$$w_{l,k} = -h_k + e^{-2\pi^2 l^2\sigma^2} \int_{S^1} h(\psi)\, \cos(2\pi(k\psi - l v(\psi)))\, d\psi.$$

The total mass is $f_0 = 1$. Because f is real-valued, we have $\bar{f}_l = f_{-l}$. Note that the inaccuracy σ occurs in the formula for $w_{l,k}$ only in the exponential factor in front of the integral.

Numerical algorithm. System (2) leads to a very fast numerical solution algorithm for the integro-differential equation (1). We cut the Fourier transformed system (2) at some fixed bound N for the Fourier indices:

$$\dot{f}_l = \sum_{\max(0,l)-N\le k\le N+\min(0,l)} w_{l,k}\, f_k f_{l-k} \quad \text{for} \quad -N \le l \le N,$$

and we increase N if for the higher Fourier coefficients f_l with $N < |l| \le 2N$ the growth $\dot{f}_l = \sum_{\max(0,l)-N\le k\le N+\min(0,l)} w_{l,k}\, f_k f_{l-k}$ is larger than some small error.

Eigenvalues of the linearization. From formula (2) we easily read off the eigenvalues of the linearization of (1) at the homogeneous solution $f = 1$:

$$\begin{aligned} c_l &= w_{l,0} + w_{0,l} \\ &= -1 - h_l + 2e^{-2\pi^2 l^2\sigma^2} \int h(\psi)\, \cos(\pi l\psi)\, \cos(2\pi l(v(\psi) - \tfrac{1}{2}\psi))\, d\psi, \end{aligned}$$

where we have used the trigonometric addition formula for the cosine. Since $c_l \to -1$ for $l \to \infty$, only finitely many eigenvalues can become unstable (i.e. positive). This holds true even for the limiting case $\sigma = 0$ if v is continuously differentiable and the points ψ such that $v'(\psi) = 0$ or $v'(\psi) = 1$ are isolated; because then the integral tends to 0 for $l \to \infty$.

Figures 2 shows stationary solutions of (1) where only first (c_1 and c_{-1}), second (c_2 and c_{-2}) and fourth eigenvalues (c_4 and c_{-4}) are unstable, respectively. Thus, Figure 2 shows (from left to right) unidirectional bundling (with $v(\psi) = \frac{1}{2}\,\psi, h = 1$), bidirectional bundling in the middle (with $v(\psi) = \frac{1}{2}\,\psi$ on $]-\frac{1}{4}, \frac{1}{4}[$, continued $\frac{1}{2}$-periodically, $h = 1$), and orthogonal arrangement (with $v(\psi) = -\frac{1}{8\pi}\sin(4\pi\psi)$ also $\frac{1}{2}$-periodic, but with $h(\psi) = \frac{1}{2}\big(G_\tau(\psi - \frac{1}{4}) + G_\tau(\psi + \frac{1}{4})\big)$, $\tau = 0.06$). The underlying optimal turning angle is sketched below each figure.

3 Hysteresis and Periodic Solutions

3.1 Codimension 1 Bifurcations

The examples above show that orientational aggregation is possible. However, if the inaccuracy is large, then inhomogeneities are smeared out by a diffusion-like

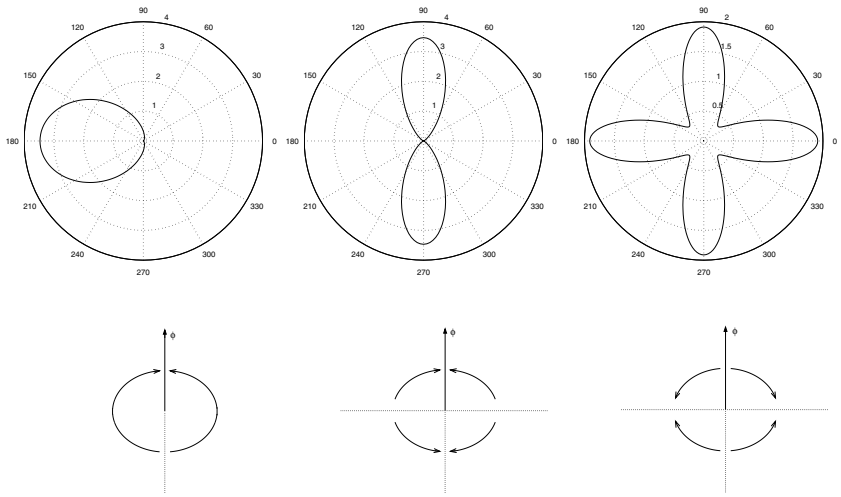

Fig. 2. Stationary solutions (upper row) and underlying optimal turning angle for equation (1). From left to right: a unidirectional bundle for $\sigma = 0.08$, a bidirectional bundle for $\sigma = 0.04$ and an orthogonal network for $\sigma = 0.02$ (parameter functions are given in the text). Depicted are polar plots in which the radius represents density $f(\theta)$.

mechanism, i.e. that for large times any solution converges to the constant solution $f = 1$ in L^2-norm. This is proved in [5] under some restricting assumptions on the interaction rate h; the statement holds e.g. for $h = 1$ or for periodic Gaussians.

It is now interesting to see how non-trivial solutions branch off the trivial solution, e.g. when the inaccuracy σ is decreased. If a single eigenvalue becomes unstable, then there is a pitchfork bifurcation which is either forward or backward. Examples for both types have been found, see [7] and Figure 3. Forward bifurcations are the rule, while backward bifurcations are rare. In the latter case a single (modulo rotation) unstable stationary solution branches off; in a secondary saddle-node-bifurcation a stable stationary solution appears, see Figure 3. The stable branch can be computed numerically (using the algorithm following equation (2)), the unstable branch in Figure 3 comes from a power series expansion based on a Lyapunov-Schmidt reduction, namely $f_l = \sum_{k \geq l} a_{l,k} f_1^k$ and $|f_1|^2 = \sum_{m \geq 1} b_m \lambda^m$, where $\lambda = \sigma - \sigma_{\text{crit}}$ is the bifurcation parameter. There is no obvious way to get it numerically — reversing time will not help, since there are infinitely many other directions in which this branch is stable.

In fact, the power series in the Lyapunov-Schmidt reduction converge, see [7]. One has to assume that the parameter functions h, v and σ depend analytically on a bifurcation parameter λ (e.g. $\sigma - \sigma_{\text{crit}}$), that $c_1(0) = 0$, $\frac{d}{d\lambda} c_1(0) = 0$, and that $|c_l(\lambda)| \geq \gamma > 0$ for $k \neq \pm 1$, λ small. Our proof that the series $f_l(f_1)$ ($l \geq 2$) converge is based on the fact that the series coefficients can be calculated via an (explicitly given) recursion formula and can be bounded from above. This bound

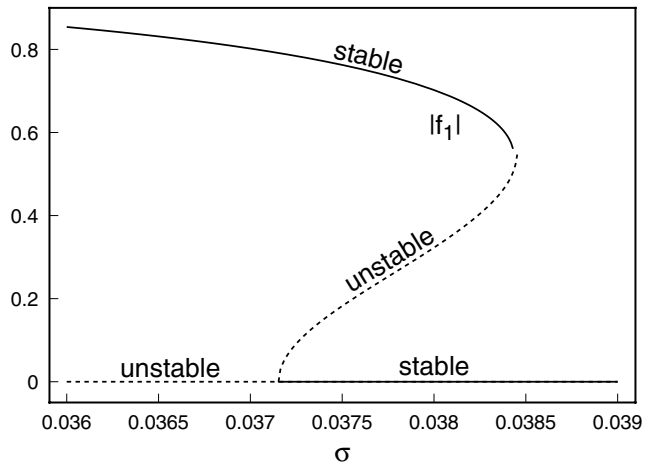

Fig. 3. Pitchfork bifurcation of an unstable branch from the constant solution and the secondary saddle-node-bifurcation. We use $v(\psi) = \frac{1}{2}\,\psi$ for $|\psi| < \frac{1}{6}$, $v(\psi) = 0$ otherwise, and $h(\psi) = 1$. For these values of σ higher eigenvalues than the first are unstable. Shown is the modulus of the first Fourier mode f_1.

yields a new system of fixed point equations. An Ansatz for solutions of the latter leads (unfortunately) not to solutions but to a second system of inequalities. Now, convergent solutions for these can be found and are upper bounds for the original series; the claim follows from this. The proof that the series $f_1(\lambda)$ converges works in a similar way but is even more technical.

3.2 Codimension 2 Bifurcations

The dynamics get more interesting when there are more eigenmodes that become unstable. If this happens at nearby points in parameter space, both bifurcations interact, and we get a great variety of different kinds of solution branches, see [3]. We assume that the first and second modes become unstable and perform a Lyapunov-Schmidt reduction. To do this we have to make some genericity assumptions similar to these for codimension one bifurcations (remember that c_l is the l-th eigenvalue of the linearization of (1) near the constant solution):

1.) h, v, σ depend analytically on two bifurcation parameters λ, μ.
2.) $c_1(0,0) = c_2(0,0) = 0$, and $\nabla_{\lambda\mu}\, c_1(0,0)$, $\nabla_{\lambda\mu}\, c_2(0,0)$ are independent.
3.) $|c_k(\lambda,\mu)| \geq \gamma > 0$ for $k \neq \pm 1, \pm 2$, (λ,μ) small.

We expand higher Fourier modes f_l (for $l \geq 3$) as power series in f_1, $\bar{f}_1$, f_2, $\bar{f}_2$ and the bifurcation parameters near the point where both eigenvalues vanish. Since solutions are invariant to turnings, the l-th series contains only terms of the form

$$f_1^{j_1}\,\bar{f}_1^{\,k_1}\,f_2^{j_2}\,\bar{f}_2^{\,k_2} \text{ where } j_1 - k_1 + 2j_2 - 2k_2 = l.$$

The first few coefficients of f_3, f_4 can be calculated explicitly when we plug the series into the stationary equations (2). Then, we substitute the power series back to get the reduced (complex) two-dimensional system of ODEs corresponding to the Lyapunov-Schmidt reduction:

$$\dot{f}_1 = c_1\, f_1 + \alpha_1\, \bar{f}_1 f_2 + \alpha_2\, f_1 |f_2|^2 + texthigherorderterms$$
$$\dot{f}_2 = c_2\, f_2 + \beta_1 f_1^2 + \beta_2\, |f_1|^2 f_2 + \beta_3\, f_2 |f_2|^2 + \text{higher order terms}$$

where

$$\alpha_1 = (w_{1,-1} + w_{1,2}), \quad \alpha_2 = -\frac{1}{c_3}\,(w_{1,-2} + w_{1,3})\,(w_{3,1} + w_{3,2}),$$
$$\beta_1 = w_{2,1}, \quad \beta_2 = -\frac{1}{c_3}\,(w_{2,-1} + w_{2,3})\,(w_{3,1} + w_{3,2}),$$
$$\beta_3 = -\frac{1}{c_4}\, w_{4,2}\,(w_{2,-2} + w_{2,4}).$$

From this reduced system, we can again get the bifurcating branches as (convergent) power series in the bifurcation parameters. In this instance, however, we have not really done the full power series expansions.

The dynamics near the codimension two bifurcation point is determined by the first few coefficients in the expansions of $\dot{f}_1$ and $\dot{f}_2$. The most important distinction is whether α_1 and β_1 have opposite signs or not, see [3]. An example for the latter case (same sign) is easy to find: one adds unipolar and bipolar bundling activity linearly. The results are biologically interesting: They show that transitions between unipolar and bipolar bundles are either via the homogeneous state (i.e. bundles dissolve and then aggregate anew) or via a mixed mode state which is neither unipolar nor bipolar (see Figure 4 for characteristics of a mixed mode solution although in a different model). Moreover, it becomes obvious that backward bifurcations (i.e. hysteresis) are a common phenomenon for non-constant interaction rate h (recall Figure 3 where $h = 1$ and the hysteresis effect is tiny).

If α_1, β_1 have opposite signs, there are much more different and interesting solutions. This is illustrated by the following example where $v(\psi) = \frac{1}{2}\psi$ for $\psi < \frac{1}{2}$ is attracting and $h(\psi) = \frac{1}{2}\,(G_\tau(\psi + 0.2) + G_\tau(\psi - 0.2))$ is maximal at interaction angles ± 0.2. At $\sigma \approx 0.103$ and $\tau \approx 0.033$ first and second eigenvalue are zero. Along with uni- and bipolar bundles and mixed mode solutions, we find traveling waves, modulated waves, oscillating bundles, and standing waves, see Figures 4 and 5. Because the equation is mirror symmetric, waves can move to the left (counter clockwise) or to the right (clockwise). Note that some of the patterns are clearly seen only for very large times (simulations have been started with some unstructured, randomly chosen distribution). In [7] a map of stable solutions near the codimension 2 bifurcation is given. It shows that oscillating bundles and traveling waves are the most common types of periodic solutions. One can also find a list of bifurcation types there.

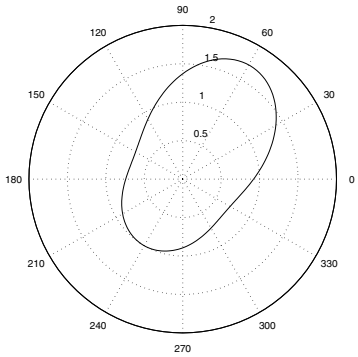

Fig. 4. A mixed mode solution for parameters $\sigma = 0.105$ and $\tau = 0.0315$.

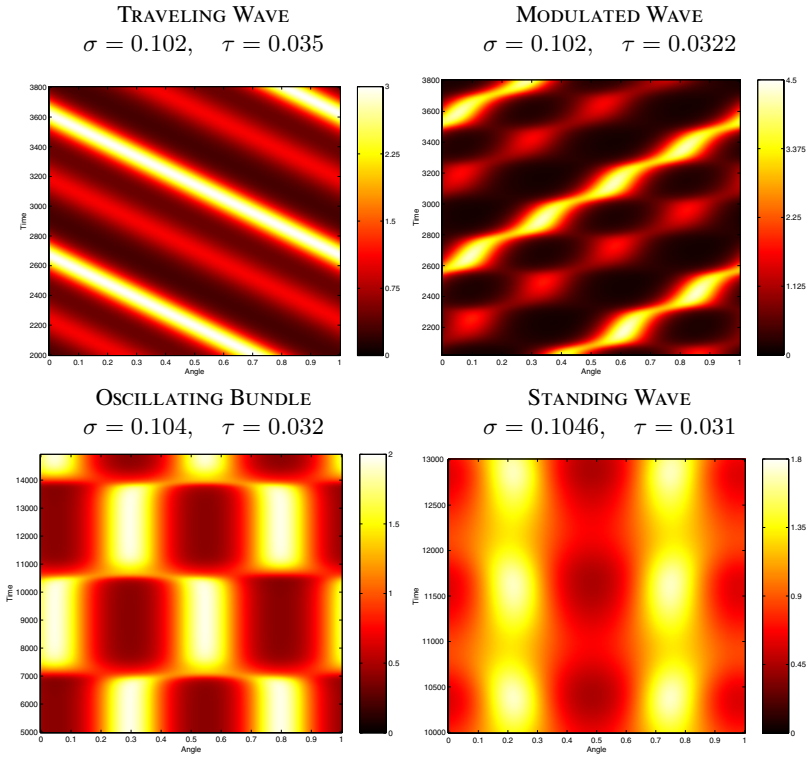

Fig. 5. Various kinds of periodic solutions near the codimension 2 bifurcation. Shown is angle θ versus time; the density is color coded, where the code is given in color bars on the right hand side. (cf. color plate 11, Page 669)

4 Peak Solutions

We call the optimal turning angle *attracting* if $0 < v(\psi) < \psi$ for $0 < \psi < \frac{1}{2}$, i.e. after turning the angle between two filaments is, on the average, narrower. If v is attracting, one can show that the first eigenvalue becomes positive for decreasing inaccuracy σ and one observes stable, unipolar stationary solutions (in some cases among other stationary solutions).

When σ tends to zero, these peaks become narrower. It is therefore natural to conjecture that in the limiting case $\sigma = 0$, there is a delta peak solution which is stable. For small σ, one can use an approximation by considering equation (1) on the real line instead of the circle (but still with functions f of unit mass). Then an exact Gaussian peak solution can be found that fits perfectly with the numerical data when σ is fairly small, see [4].

In order to approach the stability conjecture, we have to give sense to the limiting case. We write out the double integrals in (1) and perform some substitutions to get:

$$\dot{f}(\theta) = -(h * f)(\theta)\, f(\theta) + G_\sigma * \int_{S^1} h(\psi)\, f(\theta - v(\psi)) f(\theta + \psi - v(\psi))\, d\psi$$

Finally we replace G_σ by the delta distribution, i.e. we let $\sigma \to 0$, and get the limiting equation:

$$\dot{f}(\theta) = -(h * f)(\theta)\, f(\theta) + \int_{S^1} h(\psi)\, f(\theta - v(\psi)) f(\theta + \psi - v(\psi))\, d\psi. \qquad (3)$$

Note that in the Fourier transformed system (2), we only have to replace the exponential factors involving σ by 1. In [6] we prove that differentiable solutions f_σ of the original equation (1) converge to differentiable solutions f_0 of (3) uniformly on $[0, T] \times S^1$ (for differentiable initial density, bounded h and differentiable v).

In order to make sense of the statement that a delta peak is a steady state solution of the limiting equation (3), we have to extend the right hand side to measures (or distributions) $f \in \mathcal{D}'$ instead of functions. We apply the integral to a test function ϕ and obtain after some substitutions a two-fold integration of f against some modified test function (now in two variables):

$$\langle \dot{f}, \phi \rangle = -\langle f, (h * f)\, \varphi \rangle + \langle f(\theta),\, \langle f(\psi), h(\psi - \theta)\, \varphi(\theta + v(\psi - \theta)) \rangle_\psi \rangle_\theta.$$

Now it is easy to show that δ is a stationary solution of the limiting equation (3). Moreover, any delta peak $\delta_\theta := \delta(. - \theta)$ is stationary because equation (3) is equivariant under rotations (as in (1)).

Now we can look at the linearization of the limiting equation (3) at such a steady state peak solution, namely δ. This means that we perturb by small measures $\tilde{f}$, where 'small' means that we can safely ignore terms which are quadratic in $\tilde{f}$. There are more assumptions to make:
i) In order to stay in the space of measures of unit mass , $\tilde{f}$ must have mass zero ((3)

is mass conserving as well as (1)).
ii) Since there is no result from interaction with filaments located exactly opposite of our peak ($v(\frac{1}{2}) = 0$ because of periodicity and oddness), we must only consider perturbations $\tilde{f}$ which have (compact) support contained in $]-\frac{1}{2}, \frac{1}{2}[$. In this case, we can use the open interval $]-\frac{1}{2}, \frac{1}{2}[$ instead of the circle as domain for our measures, and it makes sense to speak of the barycenter $\int_{-1/2}^{1/2} \tilde{f}(\theta)\, d\theta$ of a measure.
iii) It turns out that the linearized equation not only preserves mass but also the barycenter. This comes from the fact that interaction is symmetric — the probability of jumping from θ to ψ because of interaction with a filament at ϕ is the same as that of jumping from ϕ to $\phi - (\psi - \theta)$ because of interaction with a filament at θ. Hence our peak cannot be stable against perturbation with a measure of non-vanishing barycenter.

Since all shifted peaks must also be steady state solutions, the peak cannot be stable under all possible perturbations. Perturbation with a measure that has some non-zero barycenter will result in the peak being shifted to this barycenter. As it turns out, these three conditions are also sufficient for stability:

Theorem 4.1 *If the interaction is attracting, i.e.* $0 < v(\psi) < \psi$ *for* $0 < \psi < \frac{1}{2}$, *then the delta peak is a stationary solution of (3) and it is stable under perturbation by measures* $\tilde{f}$ *such that*

i) $\tilde{f}$ *has compact support in* $]-\frac{1}{2}, \frac{1}{2}[$,
ii) $\tilde{f}$ *has zero mass,* $\int_{-1/2}^{1/2} \tilde{f}(\psi)\, d\psi = 0$,
iii) $\tilde{f}$ *has vanishing barycenter,* $\int_{-1/2}^{1/2} \psi\, \tilde{f}(\psi)\, d\psi = 0$.

The Theorem is proved by writing down an explicit series development of the solution of the linearized equation. Some fairly involved manipulations then lead to the conclusion that the solution tends to zero, see [6]. Note that this stability result holds independently of in/stability of higher modes than the first.

5 Higher Nonlinearities

One might think that aggregation is strong if filaments turn to the orientation of their interaction partner, i.e. if $v(\psi) = \psi$. Actually, this is wrong: because both partners interact and turn, all solutions converge for large times to the homogeneous distribution (this is the same argument as on page 469; see also Figure 1). In fact, the integro-differential equation (1) simplifies to $\dot{f} = -f + G_\sigma * f$, which is a diffusion-like equation, and it is not difficult to prove convergence to the constant, e.g. by using Fourier transformation. Here and in the following, we assume that the interaction rate is homogeneous, $h = 1$.

Now we introduce non-symmetric interaction, namely

$$W[f](\theta, \psi) = \alpha \int_{S^1} G_\sigma(\psi - \phi)\, p(f(\phi))\, d\phi, \tag{4}$$

where $\alpha > 0$ is the rate constant and $p : \mathbb{R}_+ \to \mathbb{R}_+$, describes some non-proportional interaction of the filament at orientation θ with filaments at orientation ϕ. We use a typical sigmoid function

$$p(f) = f^2/(1 + \beta f^2),$$

At low filament density, a single filament that turns must interact with two filaments, because $p(f) \approx f^2$. At high density, differences in filament distribution at different orientations cannot be sensed by the filament, because $p(f) \approx 1/\beta$ is constant.

We rescale such that $\alpha = \beta = 1$. The eigenvalues of the linearization near the homogeneous distribution, $f = M > 0$, are

$$c_l = -p(M) + Mp'(M)\exp(-2\pi^2 l^2\sigma^2) = \tfrac{M^2}{1+M^2}\,(-1 + \tfrac{2}{1+M^2}e^{-2\pi^2 l^2\sigma^2}).$$

This shows that aggregation is now mass dependent. Only sufficiently small mass, namely $M < 1$ (for $M = 1$, $-p + Mp'$ vanishes), and decreasing inaccuracy σ lead to instability. In the following we are interested in cases with very small inaccuracy where the number of unstable eigenvalues becomes large; indeed, for $\sigma = 0$ and $M < 1$, all eigenvalues are positive ($c_l > 0$ for $|l| \neq 0$).

Theorem 5.2 *Let $\sigma = 0$, i.e. $G_\sigma = \delta$. The stationary solutions of (1) with (4),*

$$\dot f = -\int_{-1/2}^{1/2} p(f(\phi))\,d\phi\; f + M\,p(f),$$

are exactly the step functions

$$f = 0 \cdot \chi_0 + f_1 \cdot \chi_1 + f_2 \cdot \chi_2,$$

where χ_j are characteristic functions with volumes V_j, $V_0 + V_1 + V_2 = 1$,

$$\frac{p(f_1)}{f_1} = \frac{p(f_2)}{f_2} \quad \textit{and} \quad f_1V_1 + f_2V_2 = M.$$

Stationary solutions are unstable if $0 < f_1 < f_2$ or $f_1 = 0, f_2 = M/V_2 < 1$.
Stationary solutions are stable (in the space of step functions) if $f_1 = 0$ and $f_2 = M/V_2 > 1$.

For a proof, we note that the function $P : 0 \le f \mapsto p(f)/f$ is monotonically increasing for $f < 1$ and decreasing for $f > 1$. Any horizontal line, $y = p_0 \in]0, \max P[$, crosses the graph of P two times, namely in f_1 and f_2; moreover, the derivative $\dot f$ is negative below that line and positive above that line. Note that stability is a complicated concept because these stationary solutions depend only on the volumes V_j; the steps need not be connected. We use the fact that for any fixed partition the space of step functions is invariant. Then the integro-differential equation can be reduced to a finite system of ordinary differential equations. Stability holds for any such system with appropriate, i.e. fine enough, steps.

For small inaccuracy σ stationary solutions (in numerical simulations) consist of areas with equal density which are bounded by steep (continuous) descents to 0. To approximate these transitions layers we use a Kramers–Moyal–approximation of equation (1) with (4):

$$\dot{f} = -\int_{-1/2}^{1/2} p(f(\phi))\, d\phi\, f + M\, p(f) + \tfrac{M}{2}\,\sigma^2\, p(f)'',$$

which results from the fact that for small deviation the periodic Gaussian can be approximated on $]-1/2, 1/2[$ by $G_\sigma \approx \delta + \frac{\sigma^2}{2}\delta''$. The substitution $y = p(f)$ and rescaling with $x = \frac{\sigma^2}{2}\theta$ lead to a second order ordinary differential equation:

$$y'' = c\sqrt{\frac{y}{1-y}} - y \qquad \text{where} \qquad c = \frac{1}{M}\int_{-1/2}^{1/2} p(f(\phi))\, d\phi.$$

To find the heteroclinic orbit with $y'(0) = y'(\infty) = 0$ and $y(0) = 0$ we use the energy functional $E(y, y') = \frac{1}{2}(y^2 + y'^2) - c\int_0^y \sqrt{\eta/(1-\eta)}\, d\eta$. We get $f \approx 1.515$ for the density of aggregates and $V = M/f \approx M/1.515$ for the entire volume of the aggregate. These values and the (numerically calculated) transition layer coincide very well with the results of simulations.

Thus, for small inaccuracy the integro-differential equation is basically a reaction-diffusion-system in which the diffusion term comes from the deviation from the optimal orientation (v) and the reaction term is due to interaction and turning. The diffusion not only smoothes the boundaries of homogeneous aggregates but also determines their density. In the original equation (1) numerical simulations lead to several peak-like aggregation centers when turnings take a filament almost to the interaction partner (e.g. $v(\psi) = (1-\kappa)\psi$ with $0 < \kappa \ll 1$) and $\sigma \ll 1$, see [5]. Similarly, non-symmetric and non-saturating interaction, $p(f) = f^2$, leads to peak formation at small inaccuracy. With saturation, these peaks are flattened out to aggregation areas with homogeneous density in the interior. The basic reason is that the turning rate $W[f](\theta, .)$ is (more or less) constant toward all orientations where filament density is high enough.

6 Discussion

We have presented a fairly complete analysis of a jump process with a linear jump rate on the circle. Bifurcation analysis, based on the invariance to turning (i.e. $O(2)$-symmetry), is used to analyze the emergence of aggregates (i.e. non-homogeneous solutions), to find hysteresis (i.e. backward bifurcations), and to construct all kinds of time-periodic solutions. The existence of the latter was by no means obvious. Bifurcation analysis as well as linear stability analysis of the constant solution are

based on spectral decomposition. Thus, they are restricted to systems with $O(2)$-symmetry. This is not the case for the linear stability analysis of a peak which was performed in Section 4. This method is more generally applicable because there are methods for solving linear equations, e.g. using semigroup theory. In the final section we have given an example of a jump process with a sigmoid jump rate. This leads to step function-like solutions whose stability can be clarified and which can be approximated by reducing the integro-differential equation to a partial differential equation. Thus it has become quite clear that these integro-differential equations share similarities with ordinary differential equations — many methods are applicable to both kinds of equations — as well as with partial differential equations.

References

1. Alberts, B., Bray, D., Lewis, J., Raff, M., Roberts, K., Watson, J.D. (1994): Molecular Biology of the Cell. Third Edition. Garland Publishing Inc., New York and London
2. Civelekoglu, G., Edelstein-Keshet, L. (1994): Modeling the dynamics of F-actin in the cell. Bull. Math. Biol., **56**, 587–616
3. Dangelmayr, G. (1986): Steady-state mode interaction in the presence of $O(2)$–symmetry. Dyn. Stab. Sys., **1**, 159–185
4. Geigant, E., Ladizhansky, K., Mogilner, A. (1999): An integro–differential model for orientational distributions of F-actin in cells. SIAM J. Appl. Math., **59**, 787–809
5. Geigant, E. (1999): Nichtlineare Integro–Differential–Gleichungen zur Modellierung interaktiver Musterbildungsprozesse auf S^1. PhD Thesis, Rheinische Friedrich-Wilhelms-Universität, Bonn
6. Geigant, E. (2000): Stability of a peak solution to an orientational aggregation model. In: Fiedler, B., Gröger, K., Sprekels, J.: Differential Equations. World Scientific, Singapore
7. Geigant, E., Stoll, M. (2002): Bifurcation analysis of an orientational aggregation model. Submitted to J. Math. Biol.
8. Jäger, E., Segel, L. (1992): On the distribution of dominance in populations of social organisms. SIAM J. Appl. Math., **29**, 33–58
9. Mogilner, A., Edelstein-Keshet, L. (1995): Selecting a common direction I: How orientational order can arise from simple contact responses between interacting cells. J. Math. Biol., **33**, 619–660
10. Mogilner, A., Edelstein-Keshet, L., Ermentrout, G.B. (1996): Selecting a common direction II: Peak-like solutions representing total alignment of cell clusters. J. Math. Biol., **34**, 811–842
11. Mogilner, A., Edelstein-Keshet, L. (1996): Spatio–angular order in populations of self-aligning objects: Formation of oriented patches. Physica D, **89**, 346–367
12. Othmer, H., Dunbar, S., Alt W. (1988): Models of dispersal in biological systems. J. Math. Biol., **26**, 263–298
13. Spiros, A., Edelstein-Keshet, L. (1998): Testing a model for the dynamics of actin structures with biological parameter values. Bull. Math. Biol., **60**, 275–305